Materials Science-Poland, 39(3), 2021, pp. 371-382
http://www.materialsscience.pwr.wroc.pl/
DOI: 10.2478/msp-2021-0030

sciendo

Synthesis of a novel UV-curable prepolymer 1,3-bis[(3-ethyl-3-methoxyoxetane)propyl]tetramethyldisiloxane and study on its UV-curing properties

Cheng Chen[1], Bi-Wu Huang[1,*], Zheng-Ting Lu[1], Yang Wu[1]

[1]School of Materials Science and Engineering, Nanchang University, Nanchang, 330000, Jiangxi Province, China

Precursor 3-ethyl-3-hydroxymethyloxetane was synthesized with trihydroxypropane and diethyl carbonate as the main raw materials. Intermediate 3-ethyl-3-allylmethoxyoxetane was synthesized with 3-ethyl-3-hydroxymethyloxetane and allyl bromide. Prepolymer 1,3-bis[(3-ethyl-3-methoxyoxetane)propyl]tetramethyldisiloxane was synthesized with 3-ethyl-3-allylmethoxyoxetane and 1,1,3,3-tetramethyldisiloxane. Cationic photoinitiator triarylsulfonium hexafluoroantimonate of 3 wt% was added to the prepolymer, and a novel kind of photosensitive resin was prepared. Structures of the compounds obtained at individual stages of the synthesis were analyzed and characterized by FTIR and ^{1}H-NMR. Photo-DSC analysis showed that the prepolymer had excellent photosensitivity. Thermogravimetric analysis (TG) revealed that the ultraviolet (UV)-cured samples owned excellent thermal stabilities of up to 405°C. And the mechanical properties of the UV-cured samples were tested by the universal material testing machine, giving 25.95 MPa of tensile strength, 2,935.15 MPa of elastic modulus, and 4.09% of elongation at break.

Keywords: *prepolymer, 3-ethyl-3-allylmethoxyoxetane, photo-DSC analysis*

1. Introduction

In recent decades, ultraviolet (UV) curing technology has developed rapidly and attracted much attention. Scholars like Decker [1], Shirai [2], and He [3] have done a lot of basic studies on UV curing technology. UV curing technology has the characteristics of fast curing speed, excellent properties after curing and less pollution. Therefore, it has acquired significant importance in various industrial applications, such as coatings [4], inks, electronic products, 3D printing [5, 6], and other fields. Based on previous studies [7, 8], UV curing technology mainly had two curing mechanisms: free radical polymerization and cationic polymerization. Cho [9] and Temel [10] claimed that free radical polymerization had the advantages of fast speed, easy adjustment of cured film properties, and more monomer types. But it also had many disadvantages, such as large volume shrinkage, poor adhesion, and can be easily blocked by oxygen, which greatly limited its application in certain fields. However, according to Sipan [11] and Noè [12], cationic polymerization had the advantages of low-volume shrinkage, strong adhesion, wear resistance, and high hardness and was especially suitable for 3D printing with precision requirements.

Previous literature [13, 14] reported that prepolymers commonly used in cationic UV curing systems were cycloaliphatic epoxy compounds and oxetane derivatives. Compared with cycloaliphatic epoxy compounds, oxetane derivatives had advantages of low viscosity, low toxicity, low volatility, and low synthesis cost. But they also had the disadvantage of poor photosensitivity, which limited their further development and application.

Heilen [15] had done a lot of research on silicon materials. In his book, he described that silicone materials had advantages of excellent physical and chemical properties, good temperature resistance, electrical insulation, low surface energy, and oxidation resistance. Silicone polymers also had excellent mechanical properties and thermal stability. Since Rhone Poulenc [16] synthesized UV-

* E-mail: 2258845296@qq.com

© 2021. This is an open access article distributed under the Creative Commons Attribution-NonCommercial-NoDerivatives 4.0 License. (http://creativecommons.org/licenses/by-nc-nd/4.0/)

Table 1. Materials and reagents.

Materials and reagents	Purity (%)	Manufacturer
Diethyl carbonate	99.7	Sinopharm Chemical Reagent Co., Ltd
Trihydroxypropane	99.7	Sinopharm Chemical Reagent Co., Ltd
Anhydrous magnesium sulfate (solid)		Sinopharm Chemical Reagent Co., Ltd
Potassium hydroxide (solid)		Tianjin Damao Chemical Reagent Factory
Allyl bromide	99.7	Tianjin Damao Chemical Reagent Factory
Toluene	99.9	Xilong Chemical Co., Ltd
Dichloromethane	99.7	Xilong Chemical Co., Ltd
Tetrabutylammonium bromide	99.7	Xilong Chemical Co., Ltd
Triarylsulfonium hexafluoroantimonate (UV-6976)	99.7	Dow Union Carbide
1,1,3,3-tetramethyldisiloxane	99	Shanghai Chuqing New Material Co., Ltd.
Karstedt catalyst	99.5	Shanghai Aladdin Technology Co., Ltd.
E-51 epoxy resin	98	Shanghai Resin Factory
2021p alicyclic epoxy resin	98	Daicel (China) Investment Co., Ltd

curable silicone-modified acrylate in 1979, more and more people have begun to study the subject of combining UV-curable resins with silicone materials. In recent years, some scholars, such as Piotr Murasa [17] and Zhouhui Yu [18], modified aliphatic epoxy resins with silicone. The research results showed that the two phases had good compatibility. And the introduction of a flexible Si-O bond, the toughness, moisture resistance, and thermal stability of the resin was well maintained. However, there were few literature about the modification of oxetane with organic siloxane so far.

In this paper, the 3-ethyl-3-allylmethoxyoxetane and 1,1,3,3-tetramethyldisiloxane were selected as raw materials to prepare a novel silane-modified oxetane photosensitive prepolymer. Photoinitiator triarylsulfonium hexafluoroantimonate of 3 wt% was added to the prepolymer. And after UV curing, a series of UV-cured materials were prepared. FTIR and ^{1}H-NMR were used to confirm the structures of the compounds obtained at individual stages of the synthesis. The tensile properties and thermal properties of the cured products were tested. The photosensitivity of the cured products was also analyzed by photo-DSC.

2. Experiments

2.1. Materials

The materials used in experiment were shown in Table 1.

2.2. Synthesis of 3-ethyl-3-hydroxymethyloxetane and 3-ethyl-3-allylmethoxyoxetane

Figure 1 was the synthesis route of 3-ethyl-3-hydroxymethyloxetane and 3-ethyl-3-allylmethoxyoxetane. In an alkaline environment, trihydroxypropane and diethyl carbonate underwent a transesterification reaction to synthesize a six-membered cyclic carbonate, which was then cracked at high temperature to remove CO_2. The fraction of 130–135°C/21.5 kPa was collected by vacuum distillation to obtain 3-ethyl-3-hydroxymethyloxetane. The 3-ethyl-3-hydroxymethyloxetane and potassium hydroxide aqueous solution was poured into a three-necked flask equipped with a magnetic stirrer, a thermometer, a dropping funnel, and a condensing reflux device. Then n-tetrabutylammonium bromide was added into the flask under thoroughly stirring. After that, allyl bromide was slowly added into the flask by controlling the dropping rate of the dropping funnel. The temperature

was set to be 0°C for 24 h to make the reaction complete. Then a certain amount of distilled water and dichloromethane were added to the reaction product, and the organic component was separated in a separatory funnel. The organic component was washed with distilled water several times. After that, the organic component was dried and filtered through anhydrous magnesium sulfate. XD-52AA rotary evaporator (Shanghai Xiande Instrument Experiment Co., Ltd.) was used to perform vacuum distillation to remove excess allyl bromide and dichloromethane. Then remaining fractions were performed vacuum distillation again to collect 55–60°C/0.3 kPa fractions. The final product obtained was 3-ethyl-3-allylmethoxyoxetane.

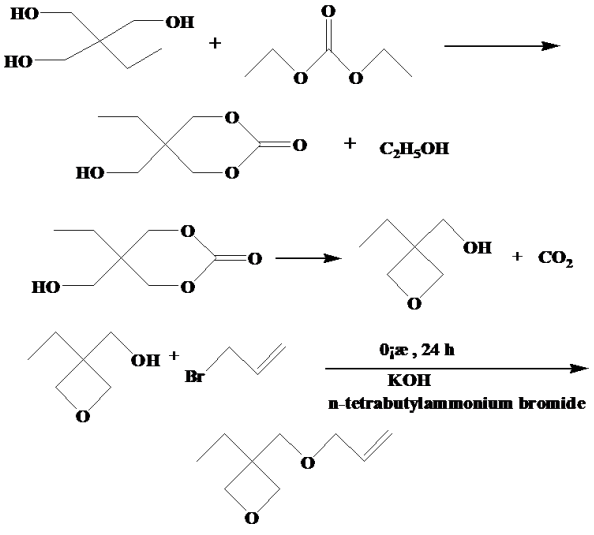

Fig. 1. Synthesis route of 3-ethyl-3-hydroxymethyloxetane and 3-ethyl-3-allylmethoxyoxetane.

2.3. Synthesis of the prepolymer

Under the catalysis of Karstedt, a hydrosilylation reaction was carried out between 3-ethyl 3-allylmethoxyoxetane and 1,1,3,3-tetramethyldisiloxane to synthesize the prepolymer. The specific reaction route was presented in Figure 2.

According to the above synthesis route, the prepared 3-ethyl-3-allylmethoxyoxetane, toluene, and Karstedt catalyst were put into a three-necked flask equipped with a reflux condenser, a thermometer, and a constant pressure dropping funnel. When the temperature rose to 80°C, 1,1,3,3-tetramethyldisiloxane dropwise was added to the three-necked flask. The reaction temperature was kept not exceeding 95°C by controlling the dropping speed of the dropping funnel. After the dripping was over, the temperature was kept at ~90 to 100°C for 5 h to obtain the crude product. Then the crude product was put into XD-52AA rotary evaporator. The temperature was increased to 100°C gradually, and then it was kept stable at 100°C for 8 h. The colorless and transparent fraction obtained was the prepolymer.

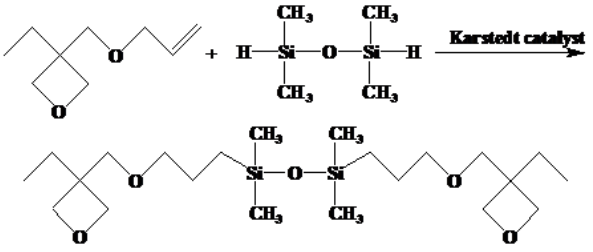

Fig. 2. Synthesis route of the prepolymer.

2.4. Characterization of the compounds

Nicolet-5700 smart Fourier Transform Infrared spectrometer (American Thermoelectric Nicolas Corporation) was used to determine whether the compounds were successfully synthesized, in the range of 400–4,000 cm^{-1} and at a resolution of 4 cm^{-1}. The liquid samples of 3-ethyl-3-hydroxymethyloxetane, 3-ethyl-3-allylmethoxyoxetane, and prepolymer were coated on the compressed KBr sheet for measurement. Infrared absorption spectrum test results were shown in Figures 4 and 5.

The 400MR DD2 Nuclear Magnetic Resonance Spectrometer (American Agilent Technologies Co., Ltd.) was used to test the ^{1}H-NMR spectra of compounds. $CDCl_3$ was chosen as solvent. Tetramethylsilane (TMS) was used as an internal reference. The experiment was operated at 600 MHz. The test results were shown in Figures 6–9.

2.5. Thermogravimetric analysis (TG) of the UV-ucred films

The most sensitive wavelength range for cationic photoinitiator triarylsulfonium hexafluoroantimonate (UV-6976) absorption was between 260 nm and 350 nm. The curing apparatus was an INTWLLI-RAY400 intelligent light-curing cabinet (Shenzhen Huishuo Electromechanical Co., Ltd, China) with 280–400 nm of wavenumber and 100 mW/cm^2 of intensity. A cationic photoinitiator of 3 wt% was added to the prepolymer. After mixing with the prepolymer evenly, the resin was put into the light-curing cabinet. After 120 s, the UV-cured films were prepared. TGA 4000 Thermogravimetric Analyzer (American PE Company) was used to analyze the thermal stability of the UV-cured films. The test was carried out in N_2 atmosphere, and the sample was weighed about 5–8 mg. The temperature of films was increased from 25°C to 800°C at a heating rate of 10°C/min, and the results were presented in Figure 10.

2.6. Viscosity test of the prepolymer

The NDJ-5 rotary viscometer (Ande Instrument Co., Shanghai, China) was used to test the viscosity of the prepolymer. The viscosity test results of the prepolymer at different temperatures were shown in Figure 11.

2.7. Photo-DSC test

The heat of the photopolymerization reaction was measured by using differential photo calorimetry DSC Q2000 (TA Instruments, New Castle, America). The light source was a mercury lamp that had a maximum intensity as high as 200 W/cm^2. The emission of spectrum radiated from this lamp was mostly between 260 nm and 450 nm. The experiment was under the nitrogen atmosphere at a flow rate of 50 mL/min. At the same time, the UV intensity was adjusted to 35 mW/cm^2, and aluminum sample pans were used. The same mass of cationic initiator was added to the prepolymer, 2021p alicyclic epoxy resin, and E-51 epoxy resin. Q2000 photo-DSC was used to test the UV curing kinetics of these three groups of formulations. The results are shown in Figures 12–14.

2.8. Mechanical property test

The same mass of cationic initiator of 3 wt% was added to the prepolymer, 2021p alicyclic epoxy resin, and E-51 epoxy resin. And the resins were stirred evenly. Then these resins were placed into an ultrasonic oscillator and shook for about 5 min.

Tensile mechanical properties test: the prepared liquid resin was poured into a polytetrafluoroethylene mold. Then the polytetrafluoroethylene mold was put into the INTWLLI-RAY400 intelligent light-curing cabinet. After being cured for 120 s, the cured samples were demolded and numbered. The dimensions of the designed samples were shown in Figure 3. After demolding, a vernier caliper was used to measure their real length, width, and thickness. Tensile samples met the standards of GB/T 1040-92 "Test Methods for Plastic Tensile Properties". Then the samples were clamped on the CMT4204 microcomputer-controlled universal material testing machine (Shenzhen New Sansi Company, China), and the tester was used to apply a tensile load to these samples along the longitudinal axis until the samples were broken. Thus the tensile mechanical properties data of the cured samples were obtained. Five identical samples were prepared, and the mechanical property test results were shown in Tables 6–8.

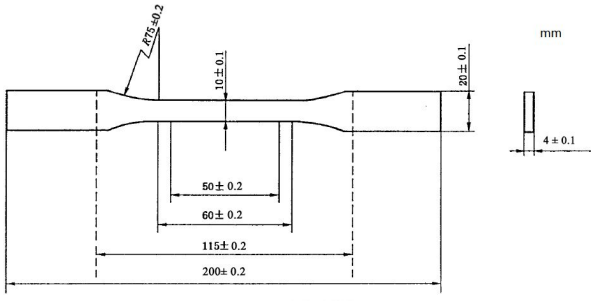

Fig. 3. Dimensions of the designed samples.

3. Results and discussion

3.1. Characterization of the compounds

3.1.1. Characterization of FTIR

The infrared spectra of 3-ethyl-3-hydroxymethyloxetane and 3-ethyl-3-allylmethoxyoxetane were shown in Figure 4. Referring to infrared analysis from H [19], in the curve of 3-ethyl-3-hydroxymethyloxetane, the wide absorption peak at 3,410 cm^{-1} corresponds to -OH. The absorption peaks at 2,960 cm^{-1}, 1,463 cm^{-1}, 2,870 cm^{-1} correspond to C-H in $-CH_3$. The absorption peaks at 2,930 cm^{-1} attributed to C-H in $-CH_2-$. The absorption peaks at 1,050 cm^{-1} attributed to C-O-C. Moreover, the absorption peak at 824 cm^{-1} belonged to the symmetric deformation vibration of the four-membered ring in oxetane, and the absorption peak at 978 cm^{-1} belonged to the antisymmetric deformation vibration of the four-membered ring in oxetane. All of the above descriptions confirmed the successful synthesis of 3-ethyl-3-hydroxymethyloxetane. In the curve of 3-ethyl-3-allylmethoxyoxetane, it could be clearly found that the absorption peak at 3,410 cm^{-1} of -OH disappeared. Absorption peaks at 3,080 cm^{-1}, 1,643 cm^{-1}, and 921 cm^{-1} attributed to the characteristic absorption peaks of the allyl group. These all indicated the successful synthesis of 3-ethyl-3-allylmethoxyoxetane.

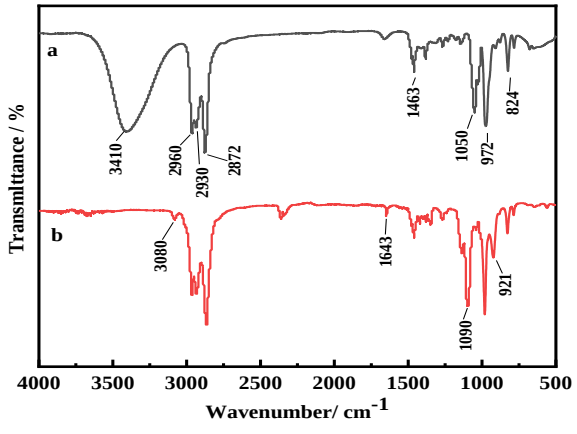

Fig. 4. **(A)** The infrared spectrum of 3-ethyl-3-hydroxymethyloxetane. **(B)** The infrared spectrum of 3-ethyl-3-allylmethoxyoxetane.

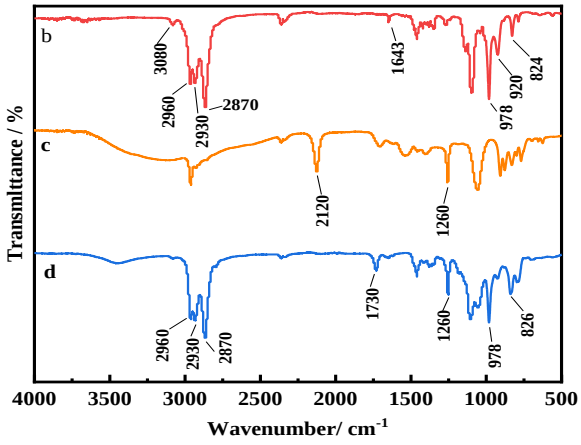

Fig. 5. **(B)** The infrared spectrum curve of 3-ethyl-3-allylmethoxyoxetane. **(C)** The infrared spectrum curve of 1,1,3,3-tetramethyldisiloxane. **(D)** The infrared spectrum curve of the prepolymer.

In Figure 5, from the curve of 1,1,3,3-tetramethyldisiloxane, the absorption peak at 2,120 cm^{-1} corresponds to Si-H, and the absorption peak at 1,260 cm^{-1} corresponds to Si-C. Comparing curves b and c, it could be found that the characteristic absorption peaks of allyl and Si-H bonds disappeared in the infrared spectrum curve d of the prepolymer, which indicated that hydrosilylation reaction between the C=C in the allyl group and the Si-H bond was complete. Meanwhile, both the characteristic absorption peaks of oxetane and Si-C appeared in the infrared spectrum of the prepolymer appeared, which further proved that the prepolymer was successfully synthesized.

3.1.2. ^{1}H-NMR analysis

The successful synthesis of 3-ethyl-3-hydroxymethyloxetane, 3-ethyl-3-allylmethoxyoxetane, and the prepolymer was determined by ^{1}H-NMR [20], which were shown in the following Tables 2–5 and Figures 6–9.

Figure 6 was the ^{1}H-NMR spectrum of 3-ethyl-3-hydroxymethyloxetane. From the Table 2, it could be seen that the ratio of the chemical shift area of H at the six positions on 1, 2, 3, 4, 5, and 6 were approximately 3:2:2:1:2:2, which complied with the ratio of the type and number of hydrogen atoms in the molecular structure of 3-ethyl-3-hydroxymethyloxetane and indi-

rectly proved the successful synthesis of 3-ethyl-3-hydroxymethyloxetane.

In Figure 6, the chemical shift of the hydrogen atom of -OH in 3-ethyl-3-hydroxymethyloxetane was at 3.74 ppm. However, it disappeared in Figure 7. It proved that the -OH in 3-ethyl-3-hydroxymethyloxetane had reacted completely. At the same time, the chemical shifts of hydrogen atoms of –CH=CH_2 in 3-ethyl-3-allylmethoxyoxetane were at 5.24 ppm and 5.87 ppm. According to Table 3, the ratio of the chemical shift area of H at eight positions was approximately 3:2:2:2:1:2:2:2, which complied with the ratio of the type and number of hydrogen atoms in the molecular structure of 3-ethyl-3-allylmethoxyoxetane and indirectly confirmed the successful synthesis of 3-ethyl-3-allylmethoxyoxetane.

Figure 8 was the ^{1}H-NMR spectrum of 1,1,3,3-tetramethyldisiloxane, it could be seen that the chemical shift of hydrogen atoms in the Si-H was at 0.17 ppm.

Comparing the Tables 4–5 and Figures 7–9, the signal of Si-H at 0.17 ppm disappeared on the ^{1}H-NMR spectrum of the prepolymer in Figure 9. The signals at 5.24 ppm and 5.87 ppm of

Table 2. Analytical table of the ^{1}H-NMR spectrum for the 3-ethyl-3-hydroxymethyloxetane.

Location of H	Chemical shift /(δ/ppm)	Structural formula
1	0.77	3H, -CH_3
2	1.60	2H, -CH_2-
3	3.58	2H, -CH_2-
4	3.74	H, -OH
5	4.28	2H, -CH_2-
6	4.33	2H, -CH_2-

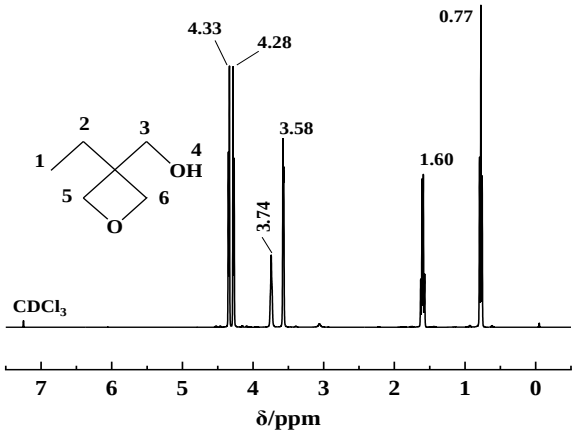

Fig. 6. ^{1}H-NMR spectrum of 3-ethyl-3-hydroxymethyloxetane.

Table 3. Analytical table of the ^{1}H-NMR spectrum for the 3-ethyl-3-allylmethoxyoxetane.

Location of H	Chemical shift/(δ/ppm)	Structural formula
1	0.86	3H, -CH_3
2	1.73	2H, -CH_2-
3	3.53	2H, -CH_2-
4	3.97	2H, -CH_2-
5	5.87	H, -CH=
6	5.24	2H, =CH_2
7	4.36	2H, -CH_2-
8	4.42	2H, -CH_2-

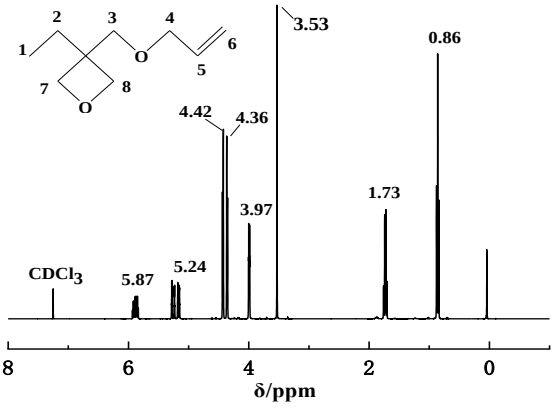

Fig. 7. ^{1}H-NMR spectrum of 3-ethyl-3-allylmethoxyoxetane.

Table 4. Analytical table of the ^{1}H-NMR spectrum for the 1,1,3,3-tetramethyldisiloxane.

Location of H	Chemical shift/(δ/ppm)	Structural formula
1	0.17	12H, -CH_3
2	4.66	2H, -Si-H

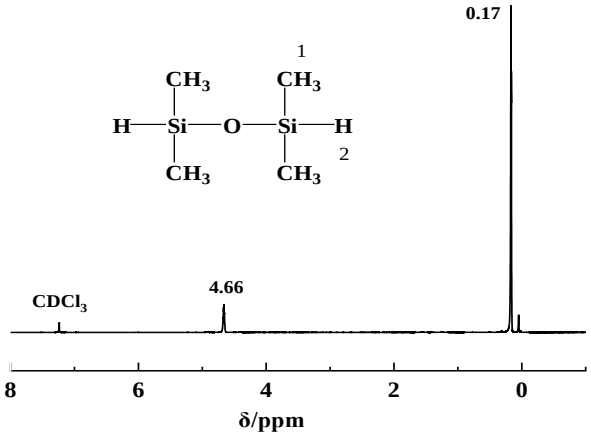

Fig. 8. ^{1}H-NMR spectrum of 1,1,3,3-tetramethyldisiloxane.

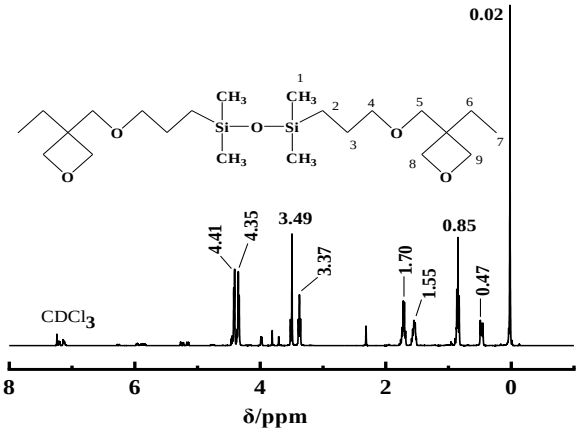

Fig. 9. ^{1}H-NMR spectrum of the prepolymer.

Table 5. Analytical table of the ^{1}H-NMR spectrum for the prepolymer.

Location of H	Chemical shift/(δ/ppm)	Structural formula
1	0.02	12H, -CH_3
2	0.47	4H, -CH_2-
3	1.55	4H, -CH_2-
4	3.37	4H, -CH_2-
5	3.49	4H, -CH_2-
6	1.70	4H, -CH_2-
7	0.85	6H, -CH_3
8	4.35	4H, -CH_2-
9	4.41	4H, -CH_2-

–CH=CH_2 in 3-ethyl-3-allylmethoxyoxetane also disappeared, which ascribed to the hydrosilylation reaction between 1,1,3,3-tetramethyldisiloxane and 3-ethyl-3-allylmethoxyoxetane. The peak area ratio of the 9 absorption peaks is 6:2:2:2:2:2:3:2:2, which confirmed the successful synthesis of the prepolymer.

3.2. TG

The thermal stabilities of films cured with prepolymer were evaluated by TG. The TG thermogram and its corresponding derivative (DTG) [21] of the prepolymer were displayed in Figure 10. As can be seen from Figure 10(a), it could be found that the mass of the cured films had little change before 100°C, indicating that the resin basically contained no moisture. The mass loss of the cured films between 100°C and 300°C was within 5%, which was related to the small amount of uncured monomer contained in the resin. Starting from about 350°C, the molecular segments of the cured films began to decompose, and the mass of the cured films declined obviously. At about 405°C, the decomposition rate [22] of the cured films reached the maximum, and then the decomposition rate gradually slowed down until the cured films were completely decomposed. The results revealed that the UV-cured films owned excellent thermal stabilities of up to 405°C.

3.3. Viscosity test results

As seen from Figure 11, the viscosity of the prepolymer decreased with the temperature increasing, which indicated that the prepolymer was a non-Newtonian liquid. Its viscosity at 25°C was only about 250 mPa/s.

The low viscosity of the prepolymer will facilitate its molding and processing in practical applications. One potential application for the prepolymer is as UV-curable material used in coating and adhesive systems. In addition, viscosity is an important criterion to balance the fluidity of a photosensitive resin in the 3D printing process. The lower viscosity of the photosensitive prepolymer is in favor of enhancing the print speed and the accuracy of the printed part.

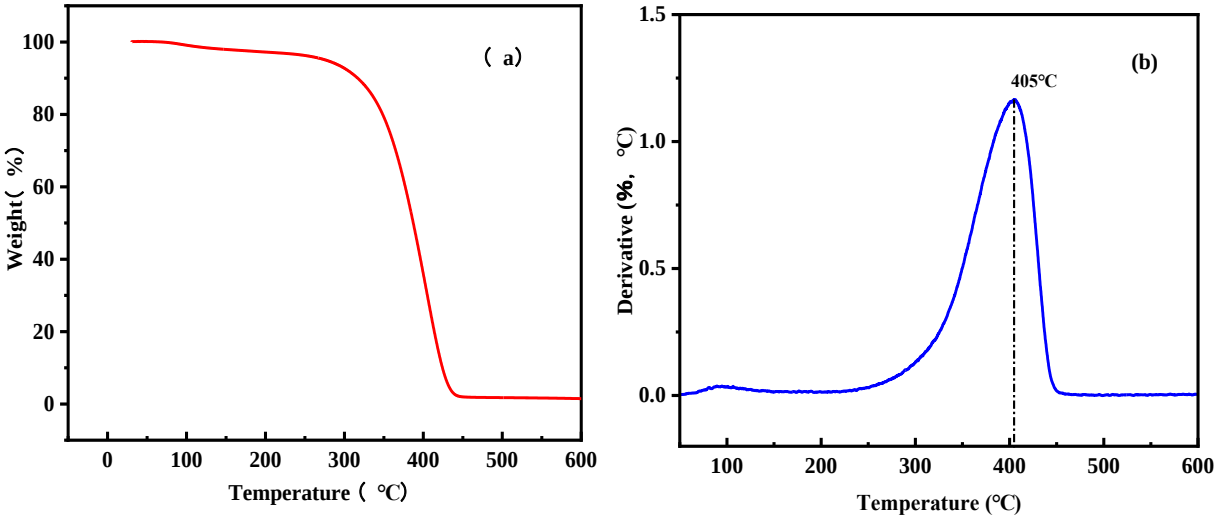

Fig. 10. TG **(A)** and DTG **(B)** curves of films cured with the prepolymer.

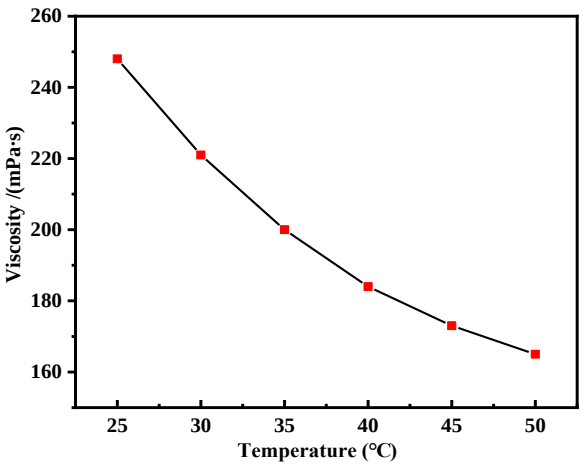

Fig. 11. The viscosity of the prepolymer at different temperatures.

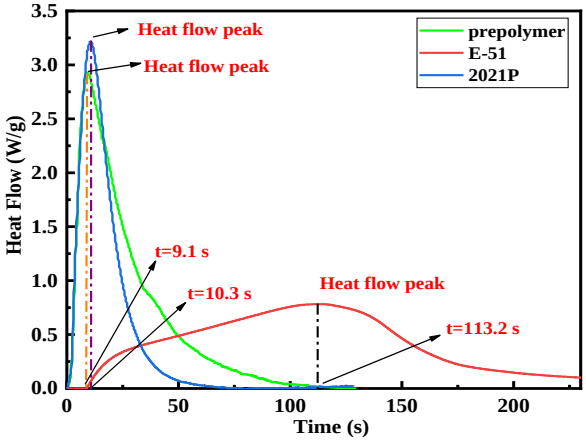

Fig. 12. Heat flow of prepolymer, E-51 and 2021p.

3.4. Photo-DSC analysis

Photo-DSC was a form of thermal analysis that provides the curing kinetics of polymerization. As shown in Figure 12, the heat flow of prepolymer, E-51, and 2021p were measured. The time for the prepolymer to reach the heat flow peak was 9.1 s, which was shorter than 2021p. However, the time for E-51 to reach the heat flow peak was much longer than the previous two, which took 103.2 s. The heat flow peak was related to the maximum reaction rate, which meant the curing rate of the prepolymer was better than that of 2021p and much better than that of E-51.

Photo-DSC provided kinetics data, taking into account that the measured heat flow rate was proportional with the polymerization rate [23]. In general, this assumption was valid only if no other enthalpic events than polymerization occur. To obtain the photo-polymerization heat (H_t) as a function of time, the heat flow rate (q) curves recorded by photo-DSC were integrated Eq. (1). This was transformed into the conversion (α) through division by the total heat of reaction (ΔH_{total}) chosen as the value obtained in the measurement at the highest

(isothermal) temperature Eq. (2).

$$Ht = \int_0^t q(t)dt, \tag{1}$$

$$\alpha t1 = \frac{1}{\Delta Htotal} \times \int_{t0}^{t1} q(t)dt. \tag{2}$$

From the total heat of the three in Figure 13, the conversion rate of the three could be calculated [24]. Figure 14 showed the conversion rate of the three in photo-polymerization. It could be seen that both the prepolymer and 2021p could reach a high conversion rate after 40 s. And the conversion rate at 120 s was close to 100%, which was better than E-51.

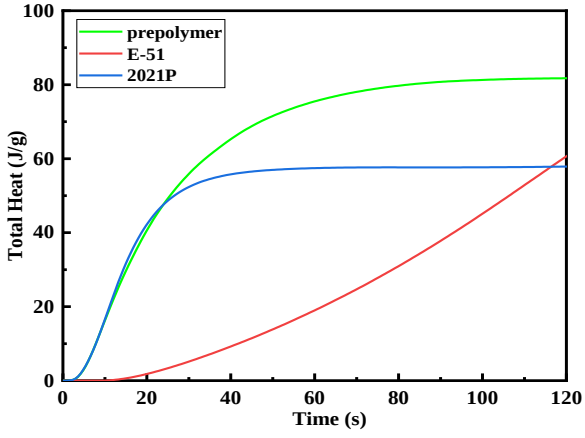

Fig. 13. Total heat of prepolymer, E-51, and 2021p.

In the experiment, if the photoinitiator was added to 3-ethyl-3-allylmethoxyoxetane, the resin would not be cured under the radiation of UV light. However, after the 3-ethyl-3-allylmethoxyoxetanesiloxane was modified with 1,1,3,3-tetramethyldisiloxane, the prepolymer could be cured and photosensitivity was improved. And from the above analysis, it was proved that the photosensitivity of the prepolymer was better than that of 2021p, which was widely used in the market. And the photosensitivity of the prepolymer was much better than that of E-51. It could be seen that the photosensitivity of oxetane was greatly improved after the modification of siloxane.

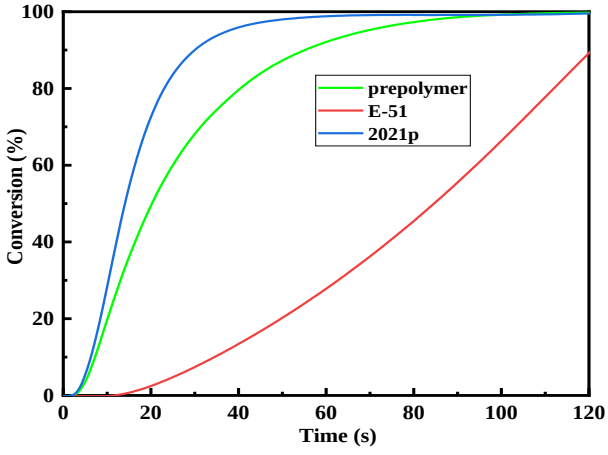

Fig. 14. Conversion of a prepolymer, E-51, and 2021p.

3.5. Mechanical property test results

Mechanical property test results of UV-cured samples were shown in Tables 6–8.

From Tables 6–8, it could be observed that the tensile strength and elastic modulus of the prepolymer and 2021p were roughly the same. However, the average elongation at break of the 2021p samples was only 2.42%, which was much worse than 4.09% of the prepolymer. The samples of 2021p were obviously brittle. Although the average elongation at break of the E-51 samples was slightly better than that of the prepolymer, the tensile strength and elastic modulus of E-51 were obviously inferior to that of the prepolymer. To sum up, among the three, the prepolymer exhibited better mechanical properties.

After the 3-ethyl-3-allylmethoxyoxetanesiloxane was modified with 1,1,3,3-tetramethyldisiloxane, the prepolymer was prepared. And after the prepolymer was cured into samples, the mechanical property test results showed good performance. The Si-O bond was introduced into the molecular chain of the prepolymer, which could increase the cross-linking network after UV curing. Thereby, the tensile strength and elongation at the break of the samples after curing were improved.

Table 6. Mechanical property test results of the prepolymer UV-cured samples.

Numbering	Tensile strength /MPa	Elastic modulus /MPa	Elongation at break /%
1	26.28	3,028.72	4.13
2	23.99	2,831.19	3.89
3	22.97	2,730.26	4.23
4	27.90	3,195.19	3.96
5	28.62	2,890.40	4.26
Average value	25.95	2,935.15	4.09
Standard deviation	2.19	161.97	0.15

Table 7. Mechanical property test results of the E-51 UV-cured samples.

Numbering	Tensile strength/MPa	Elastic modulus/MPa	Elongation at break/%
1	20.75	2,224.11	5.83
2	19.60	1,912.03	6.12
3	21.03	2,329.58	4.76
4	20.57	2,168.32	4.92
5	18.44	1,895.36	5.43
Average value	20.08	2,105.88	5.41
Standard deviation	1.06	193.53	0.58

Table 8. Mechanical property test results of the 2021p UV-cured samples.

Numbering	Tensile strength/MPa	Elastic modulus/MPa	Elongation at break/%
1	32.11	3,165.01	2.63
2	24.17	3,454.75	2.58
3	34.87	2,719.27	2.13
4	26.26	3,012.03	2.67
5	25.76	2,855.39	2.08
Average value	28.63	3,041.29	2.42
Standard deviation	4.60	285.21	0.29

4. Conclusions

Precursor 3-ethyl-3-hydroxymethyloxetane was synthesized with trihydroxypropane and diethyl carbonate as the main raw materials. Intermediate 3-ethyl-3-allylmethoxyoxetane was synthesized with 3-ethyl-3-hydroxymethyloxetane and allyl bromide. Prepolymer 1,3-bis[(3-ethyl-3-methoxyoxetane)propyl]tetramethyldisiloxane was synthesized with 3-ethyl-3-allylmethoxyoxetane and 1,1,3,3-tetramethyldisiloxane. And structures of the compounds obtained at individual stages of the synthesis were analyzed and characterized by FT-IR and ^{1}H-NMR. The results confirmed that compounds were successfully synthesized.

Cationic photoinitiator triarylsulfonium hexafluoroantimonate of 3 wt% was added to the prepolymer, and a novel kind of photosensitive resin was prepared. After UV curing, the cured samples were analyzed by thermogravimetry analysis and mechanical property test. The results showed that the cured samples had excellent thermal stability and mechanical properties. In addition, the photo-DSC analysis results revealed that the photosensitivity of the prepolymer was also outstanding.

This kind of photosensitive prepolymer ob-

tained by modifying oxetane with siloxane has never been mentioned in the previous literature. And because of the introduction of flexible Si-O bonds, the photosensitivity, thermal stability, and mechanical property of oxetane are improved. Compared with E-51 epoxy resin and 2021p alicyclic epoxy resin commonly used in the market, the synthesized prepolymer has superior properties. Because this photosensitive prepolymer has a low viscosity, there is no need to add irritating diluent to adjust its viscosity when preparing UV curable resin. So it is safe and convenient to use. In summary, excellent photosensitivity of 1,3-bis[(3-ethyl-3-methoxyoxetane)propyl]tetramethyldisiloxane meets the need of 3D printing for resin materials, which further broadens the preparation range of UV-curable products, and has certain promotion and application value.

References

[1] Decker C. Kinetic study and new applications of UV radiation curing. Macromol Rapid Commun. 2003;23(18):1067–93. https://doi.org/10.1002/marc.200290014.

[2] Shirai M. Reworkable UV curing materials. Prog Organic Coat. 2007;58(2–3):158–65. https://doi.org/10.1016/j.porgcoat.2006.08.022.

[3] Xie P, Hu L, He J, Kang W, Yang W. Mechanism and solutions of appearance defects on microfluidic chips manufactured by UV-curing assisted injection molding. J Polym Eng. 2017;37(5):493–503. https://doi.org/10.1515/polyeng-2016-0153.

[4] Sangermano M, Razza N, Crivello JV. Cationic UV-curing: Technology and applications. Macromol Mater Eng. 2014;299(7):775–93. https://doi.org/10.1002/mame.201300349.

[5] Kraft V, Schumann C, Salzmann D, Nopper H, Weyhe D, Schenk A. Towards realistic organ models for 3D printing and visualization. Curr Dir Biomed Eng. 2021;7(1):166–70. https://doi.org/10.1515/cdbme-2021-1036.

[6] Stansbury JW, Idacavage MJ. 3D printing with polymers: challenges among expanding options and opportunities. Den Mater. 2016;32(1):54–64. https://doi.org/10.1016/j.dental.2015.09.018.

[7] Zhang LJ, Wu CB, Yang F, Geng XY, Li MQ, Xiao JJ. Preparation and characterization of UV curable hybrid system based on free radical and cationic mechanism. Appl Mech Mater. 2014;470:141–45. https://doi.org/10.4028/www.scientific.net/AMM.470.141.

[8] Park YJ, Lim DH, Kim HJ, Park DS, Sung IK. UV and thermal-curing behaviors of dual-curable adhesives based on epoxy acrylate oligomers. Int J Adhes Adhesives. 2012;29(7):710–7. https://doi.org/10.1016/j.ijadhadh.2009.02.001.

[9] Cho JD, Ju HT, Hong JW. Photocuring kinetics of UV-initiated free-radical photopolymerizations with and without silica nanoparticles. J Polym Sci Part A. 2010;43(3):658–70. https://doi.org/10.1002/pola.20529.

[10] Temel G, Enginol B, Aydin M, Balta DK, Arsu N. Photopolymerization and photophysical properties of amine linked benzophenone photoinitiator for free radical polymerization. J Photochem Photobiol A. 2011;219(1):26–31. https://doi.org/10.1016/j.jphotochem.2011.01.012.

[11] Sipani V, Kirsch A, Scranton AB. Dark cure studies of cationic photopolymerizations of epoxides: Characterization of kinetic rate constants at high conversions. J Polym Sci Part A. 2004;42(17):4409–16. https://doi.org/10.1002/pola.20209.

[12] Noè C, Hakkarainen M, Sangermano M. Cationic UV-curing of epoxidized biobased resins. Polymers. 2020;13(1):89. https://doi.org/10.3390/polym13010089.

[13] Noè C, Malburet S, Milani E, Bouvet-Marchand A, Graillot A, Sangermano M. Cationic UV-curing of epoxidized cardanol derivatives. Polym Int. 2020;69(8):668–74. https://doi.org/10.1002/pi.6031.

[14] Cho JD, Hong JW. Curing kinetics of UV-initiated cationic photopolymerization of divinyl ether photosensitized by thioxanthone. J Appl Polym Sci. 2010;97(3):1345–51. https://doi.org/10.1002/app.21838.

[15] Heilen W, Herrwerth S. Silicone resins and their combinations. Hannover, Germany: Vincentz Network, 2015.

[16] Bajaj P, Gupta DC. Copolymerization of styrene and acrylonitrile with functional silanes. Eur Polym J. 1979;15(3):271–5. https://doi.org/10.1016/0014-3057(79)90175-7.

[17] Murias P, Maciejewski H, Galina H. Epoxy resins modified with reactive low molecular weight siloxanes. Eur Polym J. 2012;48(4):769–73. https://doi.org/10.1016/j.eurpolymj.2012.01.009.

[18] Yu Z, Cui A, Zhao P, Wei H, Hu F. Preparation and properties studies of UV-curable silicone modified epoxy resin composite system. J Appl Biomater Fundam Mater. 2018;16(1):170–6. https://doi.org/10.1177/2280800017753053.

[19] Huang B, Han L, Wu B, Chen H, Zhou W, Lu Z. Application of Bis[2-(3,4-epoxycyclohexyl) ethyl]octamethyltetrasiloxane in the preparation of a photosensitive resin for stereolithography 3D printing. J Wuhan Univ Technol. 2019;34(6):236–44. https://doi.org/10.1007/s11595-019-2215-7.

[20] Khalaf HI, Wady AN, Daham HK. Synthesis and characterization of new optically active poly(amide-imide)s derived from n,n′-(pyromellitoyl) bis-l-tyrosine and various diamines. Mater Sci. 2013;31(1):43–51.

https://doi.org/10.2478/s13536-012-0077-1.
[21] Altowyan AS, Ahmed HA, Gomha SM, Mostafa AM. Optical and thermal investigations of new schiff base/ester systems in pure and mixed states. Polymers. 2021;13(11):1687. https://doi.org/10.3390/polym13111687.
[22] Suresh J, Karthik S, Arun A. Photocrosslinkable polymer based on 4-(3-(2,4-dichlorophenyl)-3-oxoprop-1-enyl) phenylacrylate: Synthesis, reactivity ratio, and crosslinking studies. Mater Sci. 2016;34(4):834–44. https://doi.org/10.1515/msp-2016-0117.
[23] Shi Y, Ma W, Wang J, Mo J. 2-ethy-4-methylimidazole terminated polyurethane prepolymer as functional latent curing agents for epoxy resin crosslinking. J Macromol Sci Part A. 2019;56(8):750–8. https://doi.org/10.1080/10601325.2019.1586438.
[24] Rusu MC, Block C, Van Assche G, Van Mele B. Influence of temperature and UV intensity on photo-polymerization reaction studied by photo-DSC. J Thermal Anal Calorimetry. 2012;110(1):287–94. https://doi.org/10.1007/s10973-012-2465-5.

Received 2021-07-16
Accepted 2021-10-17